ACS OMEGA

http://pubs.acs.org/journal/acsodf

Article

# Elucidating the Interaction of Human Ferritin with Quercetin and Naringenin: Implication of Natural Products in Neurodegenerative Diseases: Molecular Docking and Dynamics Simulation Insight

Anas Shamsi,* Moyad Shahwan, Mohd Shahnawaz Khan, Fohad Mabood Husain, Fahad A. Alhumaydhi, Abdullah S. M. Aljohani, Md. Tabish Rehman, Md. Imtaiyaz Hassan, and Asimul Islam

Cite This: *ACS Omega* 2021, 6, 7922−7930

Read Online

ACCESS | Metrics & More | Article Recommendations

**ABSTRACT:** Recent research has advocated the significant contribution of metal dyshomeostasis in developing and progressing Alzheimer's disease (AD). Disruption of homeostasis creates an imbalance of the metal ions that causes neuronal dysfunction and death. Flavonoids such as quercetin and naringenin play an essential role in iron homeostasis and are widely explored in treating various complex diseases. Iron is a critical player in many physiological activities, and hence, its homeostasis is essential for the normal functioning of the brain. Iron deficiency and iron overload contribute to AD development, highlighting the importance of maintaining iron homeostasis. Ferritin is an iron protein associated with the storage and sequestration of excess ferrous iron, playing a pivotal role in maintaining iron levels. Flavonoids are the most common polyphenolic compounds present in the human diet and are known to exert multiple neuroprotective actions. Naringenin and quercetin are extensively explored polyphenols having a broad range of therapeutic potential ranging from cancers to neurodegenerative disorders. This study aims to investigate their binding, employing molecular docking and molecular dynamics (MD) simulation in light of these polyphenols' and ferritin's therapeutic importance in AD. In this study, we performed structure-based docking of quercetin and naringenin with human ferritin. First, the binding affinity of quercetin and naringenin toward ferritin was estimated, and then their close interactions were explored to find the stable poses. All-atom 100 ns MD simulations further escorted the docking study, followed by principal component and free energy landscape analyses. The dynamic studies helped investigate the conformational dynamic, structural stability, and interaction mechanism of ferritin with quercetin and naringenin. The MD analysis suggested that the binding of quercetin and naringenin with ferritin stabilizes throughout the simulation period and leads to fewer conformational deviations. This study gives an insight at the atomistic level into the interaction between quercetin and naringenin with ferritin, thereby aiding in understanding the activity and mechanism of protein and drug binding. The study is clinically significant as iron participates in the occurrence of AD.

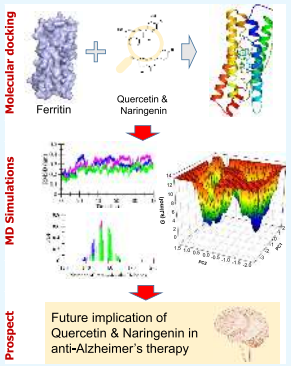




## 1. INTRODUCTION

Iron has evolved and has been incorporated in life as an essential element in numerous metabolic processes by using it in electron transfer, biochemical catalysis, storage and transport of oxygen, etc. Iron availability and adequate compartmentalization are necessary for normal human physiological functions. However, the chained process of procurement, distribution, and utilization of the metal in the cellular environment can be surplus in oxygen and reducing counterparts is at most risk.[1] The redox-active metal iron is substantially similar to potassium, sodium, zinc, and calcium as it is generally a part of single-electron transfers. Irregulated and miscoordinated iron in the labile-iron pool of cells can generate reactive oxygen species (ROS) that alter the structure of lipid, proteins, and nucleic acids, leading to immediate problems like loss of functionality, protein aggregation, and destabilization. Besides, iron can also increase the aggregation of proteins with intrinsic sequence disorders, which are generally considered the sequence for normal functions, independent of ROS modification and mutation. A few of these aggregate-prone proteins have a significant role in many neurological conditions. For example, $\alpha$-synuclein, having a normal sequence in Parkinson's disease (PD), a partially misordered stretch of amino acids is sensitive to iron levels as iron enhances its aggregation.[2,3]

Similarly, in AD, a partially disordered amyloid $\beta$ (A$\beta$) peptide undergoes aggregation in the presence of excess iron.[4] Moreover, the aggregates formed can generate ROS and

Received: January 28, 2021
Accepted: March 2, 2021
Published: March 11, 2021

induce a redox change in iron.[4,5] Both accumulation of iron and dysregulation of iron metabolism in specific regions of the brain are associated directly with several infamous neurodegenerative diseases known by the name neurodegeneration with brain iron accumulation (NIBA) diseases[6,7] and also with the more common ones.[8] The issues associated with iron homeostasis are wide; to address these inevitable issues of iron availability and potential toxicity due to improper coordination, the protein ferritin has emerged as the checkpoint protein to store or remove excess iron and control the bioavailability as required by the cells and ultimately to curb the cellular damage and stress.[9]

Ferritin molecule is a well-characterized one with two dozen protein subunits that form a shell symmetrically, which further defines a cavity that can lodge up to 4500 iron atoms.[10] In native form, human ferritin is present as a heteropolymer consisting of FTH1 (21 kDa) and FLT (20 kDa). The three functional genes of ferritin are as follows: FTH, located on the 11th chromosome, encodes a 183 aa long, cytosolic heavy chain; FLT, located on the 19th chromosome, encodes a 175 aa long cytosolic light chain; and FTMT, located on chromosome 5, encodes a 242 aa precursor of mitochondrial ferritin. The chief functions of ferritin are to stock up and sequester excess ferrous iron to maintain the normal cellular processes by keeping a halt on ROS production, iron deposition, and protein aggregation and freeing up the reserved iron required by the cellular processes.[1] Free ferrous (Fe II) iron reacts with hydrogen peroxide by the Fenton reaction, generating ROS; hence, it is destructive. It creates an oxidative stressed environment and attacks proteins, lipids, and nucleic acids. Ferritin protects cells against radicals formed by iron-mediated processes by seizing iron in an inactive redox form. The reserved iron is available as per the cellular demands. However, the regulation of iron released by ferritin needs more research to find an exact explanation. Many investigations indicate that the iron release is mediated by hydrophobic channels.[11]

Alzheimer's disease is characterized by the early loss of memory followed by language disorders, loss of direction, and excessive anxiety, becoming dominant as the condition worsens; the disease occurs mostly in elders.[12] AD is generally classified into two types: (1) early-onset/familial AD (FAD) and (2) sporadic AD (SAD).[13] Mental functions such as emotional and behavioral aspects, cognition, etc., become extremely low and miscoordinated, leading to loss of body function gradually.[14] The two significant hypotheses related to the AD development mechanism are the amyloid cascade hypothesis and neurofibrillary tangles hypothesis.[4] Recent studies have demonstrated that A$\beta$ and tau act synergistically to disrupt neural circuits that lead to cognitive decline in AD.[15] The second theory, which another group of researchers supports, correlates inflammation to metals and is known as the metal ion hypothesis, which contributes immensely to the mechanism of the disease. The inflammation theory gained the limelight because of the level of microglia and activated astrocytes in AD patients' brains together with elevated expression levels of TNF-a, IL-6, IL-1b, and other inflammatory factors.[16]

With extensive ongoing researches across the globe, it was also concluded that the steady-state dysregulation of metal ion metabolism *in vivo* is linked with AD. Imbalances in the metal levels in the AD brain were reported in various reports, which were coupled with metal-induced oxidative damage, stressing the crucial importance of metal dyshomeostasis in AD development and progression.[17,18] The association of AD with metals such as iron, copper, aluminum, zinc, and magnesium has been reported previously in the literature.[19] Metal ions can influence neuronal metabolism, promoting A$\beta$ deposition and an increase in oxidative stress.[20] AD has a multifactorial etiology, with key risk factors being age and familial background. Many epidemiological studies suggest the role of metal ions (iron homeostasis and copper), prior head injuries, and low educational status.[21] Investigations on metal homeostasis imbalances also highlight that the imbalance can lead to neuronal dysfunction and death.[22,23] Iron is a critical player in many physiological activities, and hence, its deficiency during the development of the brain leads to irreversible damage and a halt in brain development. Iron overload, on the contrary, creates a neurotoxic environment in the brain that affects normal brain function. Besides, ferritin contributes as a blood biomarker for preclinical AD.[24] Another section of literature reported high concentrations of CSF ferritin, encouraging a possibility of iron-mediated A$\beta$ deposition and progression of the disease. Excessive iron leads to A$\beta$ plaque formation in the brain; the iron load leads to hyperphosphorylated tau in the brain, a major cause of several tauopathies.[25,26]

Flavonoids are the most common polyphenolic compounds present in the human diet. They are known to exert multiple neuroprotective actions that include the ability to shield neurons against neurotoxin-induced injury[27] and to protect against neuroinflammation,[28] and are potent to enhance memory and learning and promote cognitive functions.[29] Flavonoids have been shown to enter the brain[30] and inhibit inflammatory processes carried out by glial cells.[27] Citrus fruits have been studied for their anti-inflammatory, antitumor, anticarcinogenic, and other biological activities.[31−33] The flavanone naringenin (4′,5,7-trihydroxyflavanone-7-rhamnoglucoside or naringenin-7-rhamnoglucoside) has a restricted distribution, is specific to citrus fruits, and is predominant in grapefruit, which makes up 10% of the dry weight and is responsible for the bitterness of the fruit juice.[34]

The flavanone weakens TNF$\alpha$ production and iNOS expression in glial cells, showing strong anti-inflammatory potential. Moreover, naringenin shows protective action against inflammation resulting in neuronal death in the primary neuronal co-culture system of the glial cells.[35] Naringenin is also reported to inhibit LPS/IFN-c-induced p38 mitogen-activated protein kinase (MAPK) and signal transducer and activator of transcription-1 (STAT-1), exerting an anti-inflammatory effect on the cells.[36] When compared to ascorbic acid, naringenin showed a higher protective effect against neuronal damages induced by A$\beta$ plaques.[36] The polyphenol's neuroprotective role was also studied in the 6-OHDA model of PD;[37] the compound exhibited antioxidative properties and can penetrate the brain.[38] When administered in a mouse model with induced $\alpha$-synuclein pathology, naringenin showed a decrease in neuroinflammation and $\alpha$-synuclein pathology with an increase in levels of dopamine and dopamine transporters.[39]

Quercetin, the polyphenolic compound commonly found in fruits and vegetables such as broccoli, onions, and apples, shows good antioxidant, anti-inflammation,[40] and anticancer[41] potential and has shown an excellent biological property for human health. Quercetin is well known to cross the blood−brain barrier of *in situ* models.[42] Additionally, quercetin shows


https://dx.doi.org/10.1021/acsomega.1c00527
ACS Omega 2021, 6, 7922−7930

a protective effect in induced neurodegeneration in AD.[43] Quercetin has a strong capacity to suppress the formation of Aβ fibrils and protect neuronal cells from Aβ-mediated toxicity.[44] The compound also improves catalase and superoxide dismutase activity,[45] therefore preventing glutathione depletion.[46] Moreover, it was investigated that quercetin curbs the neuronal death in the hippocampus, resulting in enhanced learning and improved memory.[47] When assembled, these chunks of evidence point out the possibility of the polyphenol quercetin exerting an effect on the central nervous system.

Here, we have explored the molecular interaction and binding mechanism of quercetin and naringenin with ferritin utilizing structure-based molecular docking and molecular dynamics (MD) simulations. The MD simulation studies, principal component analysis (PCA), and free energy landscape (FEL) analyses were performed to evaluate the structural flexibility and dynamic stability of ferritin in the presence of quercetin and naringenin. The all-atom MD simulations for 100 ns on the apo form of ferritin and its complexes with quercetin and naringenin were performed to describe their interaction and conformational changes under explicit solvent conditions. This study delivers an atomistic insight into the binding mechanism of quercetin and naringenin with ferritin utilizing state-of-the-art computational approaches.

## 2. RESULT AND DISCUSSION

**2.1. Molecular Docking.** The analysis of docking results suggests that quercetin and naringenin bind to ferritin with an appreciable affinity and make several close contacts. The selected binding poses of quercetin and naringenin show an estimated docking score with ferritin of −9.0 kcal/mol and −8.7 kcal/mol, respectively. Quercetin and naringenin show p*Ki* values of 6.21 and 5.36, respectively. They possess LE values of 0.31 and 0.29 kcal/mol, respectively, which show their good binding efficiency. The detailed interaction analysis of all generated docked conformers of both compounds (quercetin and naringenin) toward ferritin shows different close interactions. We have selected those conformers that bind with the critical residues of the ferritin binding pocket. The selected docked conformers of quercetin and naringenin show many close interactions with the ferritin binding pocket residues such as Arg22, Asn25, Tyr29, Asp89, and Ser113. The binding poses of quercetin and naringenin with ferritin and their interactions are shown in Figures 1 and 2.

The binding of quercetin and naringenin with ferritin was stabilized by many interactions which were further exploited by doing a detailed analysis. The analysis suggests that both compounds offer many interactions with the functionally important residues of ferritin. It can be seen from Figure 2 that quercetin and naringenin pointedly interact with many essential residues, including a few close contacts. Quercetin makes three hydrogen bonds with Tyr29, Asn109, and Ser113, and many other noncovalent interactions (Figure 2a). Quercetin and naringenin bind near the diiron center of ferritin, where a set of reduced flavins (RBFH2 and FMNH2) is docked and shows a similar mode of interaction.[48] The quercetin and naringenin binding residues were also found to interact with triethylene glycol (PDB ID: 5UP9) and bis(azanyl)-chloranyl-oxidanyl-platinum (PDB ID: 5N26), as discovered in their co-crystallization with ferritin. Both compounds (quercetin and naringenin) bind near Glu27 and Glu62, residues known to bind with iron.[49] Quercetin and naringenin bind into the ferritin's surface cavity with virtuous

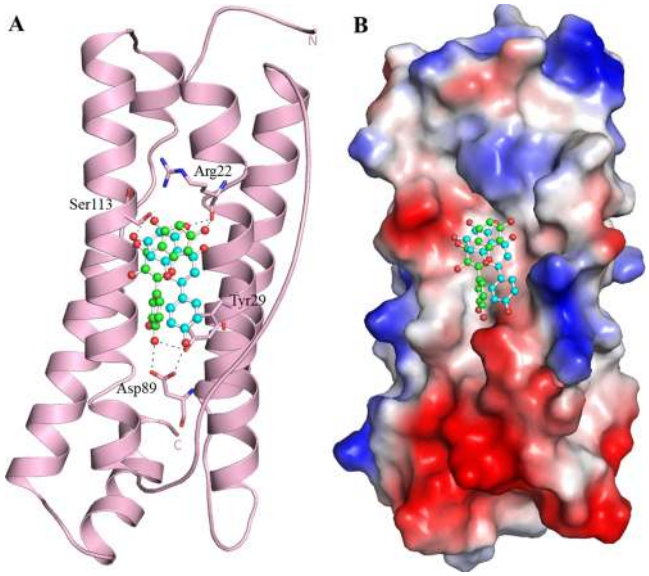


**Figure 1.** Ferritin interaction with quercetin and naringenin. (a) Cartoon diagram of ferritin showing close interactions with quercetin (green) and naringenin (cyan). (b) Electrostatic surface potential of ferritin in complex with quercetin (green) and naringenin (cyan).

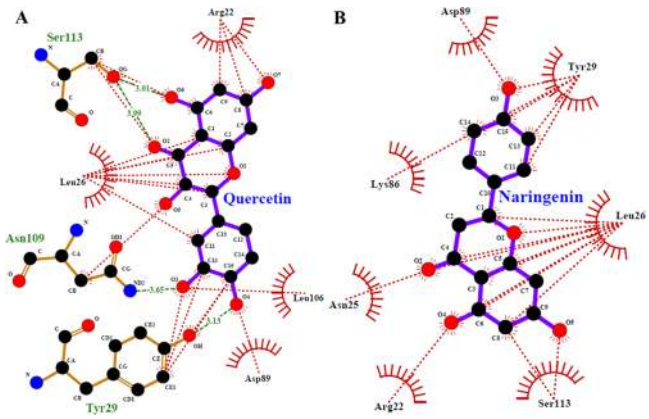


**Figure 2.** LigPlot interactions of (a) quercetin and (b) naringenin with ferritin.

complementarity (Figure 1b). Quercetin and naringenin act as good binding partners of ferritin, which can be further exploited in related medical applications.

**2.2. MD Simulations.** MD simulation methods have been utilized as an accompaniment to laboratory experiments to explore the binding mechanism and conformational behavior of proteins and their potential inhibitors. Here, to understand the structural behavior of ferritin and its interaction with quercetin and naringenin, we have performed MD simulation studies for 100 ns. First, to determine the equilibration and system stability during the simulations, we have calculated the potential energy of the apo ferritin, ferritin−quercetin, and ferritin−naringenin systems. We have estimated the potential energy for the apo form of ferritin, ferritin−quercetin complex, and ferritin−naringenin complex as −950,856, −950,742, and −950,566 kJ/mol, respectively. Other MD parameters such as RMSD, RMSF, $R_g$, SASA, etc., were also estimated after completing the simulation process (Table 1).

*2.2.1. Structural Deviations and Compactness.* Studying the root-mean-square deviation (RMSD) has allowed us to


https://dx.doi.org/10.1021/acsomega.1c00527
ACS Omega 2021, 6, 7922−7930

**Table 1. MD Parameters of the Apo Form of Ferritin and Its Complexes with Quercetin and Naringenin**

| system | RMSD (nm) | RMSF (nm) | $R_g$ (nm) | SASA ($nm^2$) | kinetic energy | volume ($nm^3$) | density (g/L) |
|---|---|---|---|---|---|---|---|
| ferritin | 0.28 | 0.15 | 1.83 | 107.66 | 152,341 | 616.89 | 1011.99 |
| ferritin−quercetin | 0.30 | 0.12 | 1.80 | 104.50 | 152,382 | 617.03 | 1012.28 |
| ferritin−naringenin | 0.24 | 0.13 | 1.82 | 107.01 | 152,346 | 616.99 | 1012.12 |

analyze the dynamic behavior, including ligand-induced conformational changes in the ferritin structure. Three MD simulations (two for ferritin complexed with quercetin and naringenin and one for the apo form of ferritin) were performed. The resulting RMSD graph was explored to assess the ligand-induced conformational changes in the ferritin structure. The average values of RMSD for apo ferritin, ferritin−quercetin complex, and ferritin−naringenin complex were found to be 0.28, 0.30, and 0.26 nm, respectively (Table 1). Figure 3a shows that quercetin and naringenin induce minimal conformational changes in the ferritin structure. A slight increment in the RMSD values of the apo form of ferritin signifies the initial structural adjustment during the simulation process. The RMSD of the ferritin−quercetin complex shows higher mobility compared with that of the apo form of ferritin and the ferritin−naringenin complex. The RMSD plot suggests that the ferritin−naringenin complex obtains less mobility since its RMSD values are lesser than those of the apo form of ferritin. The RMSD values of ferritin in the presence of quercetin and naringenin suggest no significant changes that are equilibrated without any switching throughout the simulation. Overall, the RMSD plot signifies durable stability of the ferritin−quercetin and ferritin−naringenin complexes (Figure 3a).

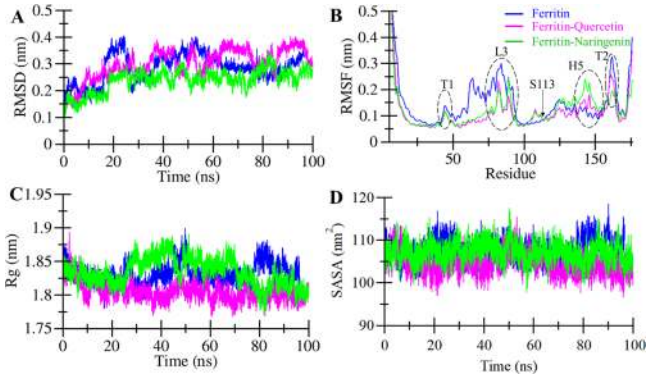


**Figure 3.** Structural dynamics and compactness of ferritin as a function of time. (a) RMSD plot of ferritin before and after quercetin and naringenin binding. (b) Residual fluctuation plot of ferritin and its docked complex with quercetin and naringenin. T1 and T2 represent turns, L3 is the loop-3 region, and H5 represents helix-5 in ferritin. (c) Time evolution of the radius of gyration. (d) SASA plot of ferritin as a function of time.

Along with the RMSD analysis, we also plotted the RMSF values generated for the apo form of ferritin and its complexes with quercetin and naringenin (Figure 3b). These RMSF values were plotted for each residue in the ferritin backbone in its apo form and after binding of quercetin and naringenin over the simulation. The RMSF plot indicates that the fluctuations of the residues are reduced for the ferritin structure while in the presence of both compounds (quercetin and naringenin) as compared to the apo form. The higher fluctuations in the case of ferritin−quercetin and ferritin−naringenin systems are related to the residues of a loop and helix region (∼aa130−aa150), while the reduced fluctuations are related to the ligand-binding site. The RMSF values are reduced when ferritin is bound to quercetin and naringenin. Overall, the RMSF plot indicated that the residual fluctuations are minimized in the region where quercetin and naringenin bind (Figure 3b).

To further comprehend the structural stability of ferritin before and after binding of quercetin and naringenin, we studied the compactness parameter of the structure by figuring the radius of gyration ($R_g$). The $R_g$ plot shown in Figure 3c demonstrates that ferritin's structural dynamics remain stable during the simulation period. The structural integrity of all three systems was intact, with average $R_g$ values for ferritin, ferritin−quercetin complex, and ferritin−naringenin complex of 1.83, 1.80, and 1.82 nm, respectively. A slight decrement in the $R_g$ values of ferritin while in complex with quercetin and naringenin signifies its stable structural dynamics. We did not observe any structural switching in ferritin in the presence of quercetin and naringenin and attained stable $R_g$ equilibrium throughout the simulation period (Figure 3c).

To examine the effect of quercetin and naringenin binding on the hydrophobic core and solvent accessibility of ferritin, we have calculated the solvent-accessible surface area[50] for the simulation trajectory. We have calculated the SASA of the apo form of ferritin, ferritin−quercetin complex, and ferritin−naringenin complex to study their conformational behavior during the simulation. There was no significant change to ferritin's SASA observed after the binding of quercetin and naringenin. The SASA values for ferritin, ferritin−quercetin complex, and ferritin−naringenin complex were estimated to be 107.66, 104.50, and 107.01 $nm^2$, respectively. The SASA for the 100 ns simulation trajectory is plotted in Figure 3d, suggesting the ferritin−naringenin complex as the apo form of ferritin with minimal changes. Overall, the SASA of ligand-bound systems seems to attain a stable equilibrium without any major peak during the simulation, signifying the stability of ferritin compactness in the presence of quercetin and naringenin.

*2.2.2. Dynamics of Intra/Intermolecular Interactions.* Hydrogen bonds (H-bonds) formed within a protein are key pillars of its structural stability.[51] H-bond analysis is used to study the stability of protein structures and their binding with different ligands.[51] H-bonds that form the primary interactions within ferritin intramolecularly are shown in Figure 4

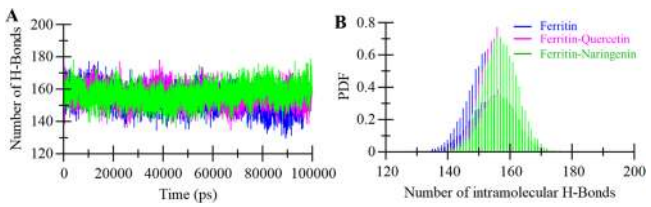


**Figure 4.** (a) Time evolution and stability of hydrogen bonds formed intramolecularly within ferritin. (b) The probability of distribution of hydrogen bonding as PDF.


https://dx.doi.org/10.1021/acsomega.1c00527
ACS Omega 2021, 6, 7922−7930

accordingly. The intramolecular H-bonding study was carried out to confirm the stability of ferritin after quercetin and naringenin binding. Here we found that quercetin and naringenin do not appear to disrupt the H-bonding within ferritin. The average numbers of intramolecular H-bond dynamics in the apo form of ferritin, ferritin−quercetin, and ferritin−naringenin were found to be 153, 156, and 156, respectively (Figure 4a). A slight increment in intramolecular H-bonding of ferritin after quercetin and naringenin binding is portentous to the higher compactness of some intramolecular space within the protein. We have also calculated the probability density function (PDF) of intramolecular H-bonds during the simulation, which displays that the complexes of ferritin−quercetin and ferritin−naringenin are quite stable during the simulation as compared with the apo form of ferritin (Figure 4b).

Furthermore, to understand whether quercetin and naringenin bind to ferritin in the same manner or not as depicted by the docking study, the intermolecular H-bonds formed between quercetin and naringenin and the residues lining the binding pocket of ferritin were calculated for the simulation trajectory. We have calculated and plotted the H-bonds formed between quercetin and naringenin with ferritin paired within 0.35 nm, suggesting the complex stability (Figure 5). The analysis shows that quercetin and naringenin bind with

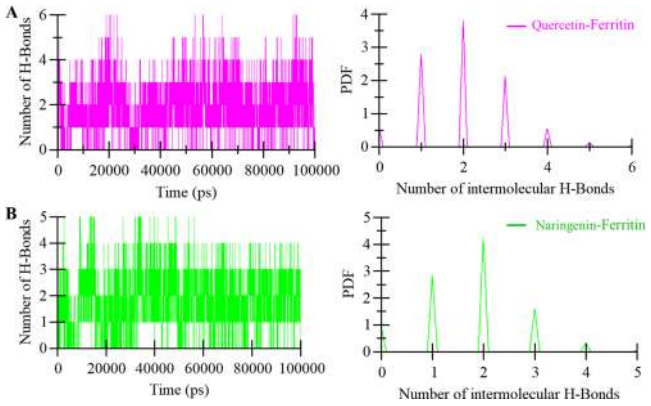


**Figure 5.** Time evolution and stability of hydrogen bonds formed intermolecularly between ferritin and (a) quercetin and (b) naringenin (right panel shows the probability of distribution of hydrogen bonds as PDF).

ferritin with four to six H-bonds with higher fluctuation and two to three H-bonds with stability throughout the simulation. We can see that two to three intermolecular interactions were shared by quercetin and naringenin to ferritin with relative stability. PDF of intermolecular H-bonds also suggests that two H-bonds are established between quercetin and naringenin and ferritin with higher distribution (Figure 5, right panels).

**2.3. Principal Component and Free Energy Landscape Analysis.** Protein function is governed by the collective atomic motions and gaining different conformations. To study the collective motion of ferritin before and after binding with quercetin and naringenin occupied in the conformational subspace during the simulation, we performed principal component analysis (PCA) by the projection of the PC1 and PC2 using the GROMACS utilities, i.e., *gmx anaeig* and *gmx covar*. The eigenvalues were extracted corresponding to each eigenvector (EV) where the EV1 and EV2 were considered by diagonalizing the covariance matrix of EVs to outline the essential subspace. The dynamic motion of ferritin in the apo form, ferritin−quercetin complex, and ferritin−naringenin complex obtained through the projection of EV1 and EV2 by the ferritin $C^{\alpha}$ atoms is illustrated in Figure 6a. The plot

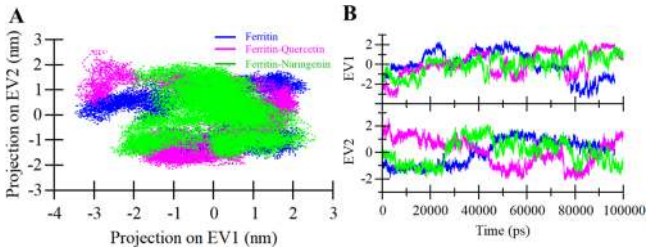


**Figure 6.** Principal component analysis. (a) Two-dimensional projections of trajectories on eigenvectors showed different projections of ferritin. (B) The projections of trajectories on eigenvectors concerning time.

shows that the ferritin−quercetin and ferritin−naringenin complexes occupied notably different conformations within the reduced subspace as compared to the free ferritin. It is outward from the PCA plot that the collective motions of the ferritin−naringenin complex are localized in a small subspace compared to the ferritin−quercetin complex. Figure 6b shows that the overall flexibility of the ferritin while in the presence of quercetin and naringenin was decreased at PC1 with a significant overlapping of stable clusters with ferritin in the apo form. The PCA analysis suggests that ferritin in complex with quercetin and naringenin is quite stable with decreased dynamics of its conformational motions.

The FELs deliver a precise portrayal of a protein's most stable conformational ensembles, which are certainly important to study the conformational changes underlying protein−ligand interactions. The FEL plots were constructed and analyzed using the first two EVs of the apo form of ferritin and its complexes with quercetin and naringenin. Figure 7 displays the FELs of ferritin, ferritin−quercetin complex, and ferritin−naringenin complex where the deeper blue indicates the stable conformational states having lower energy. Ferritin has overall a single global minimum confined within a single local basin with the lowest energy. This global minimum, in the case of the ferritin−quercetin and ferritin−naringenin complex, acquired a wider basin. The conformational ensemble derived from FEL shows that ferritin, while complexed with quercetin and naringenin, clustered in the different wider basins distributed along the PC1 compared to the apo form of ferritin. The FEL analysis suggests that the presence of quercetin and naringenin affects the size and the position of the sampled energy basin of ferritin with a stable equilibrium (Figure 7b,c).

## 3. CONCLUSIONS

To sum up, utilizing the molecular docking and MD simulation approach, we have explored the binding mechanism of quercetin and naringenin with human ferritin. We have explored their potential as lead compounds for therapeutic development against AD. *In silico* analysis using structure-based molecular docking, and dynamic simulation of quercetin and naringenin with ferritin gives an insight into their interaction mechanism. The docking results showed that quercetin and naringenin effectively bind to ferritin with many close interactions. MD simulations, PCA, and FEL analyses


https://dx.doi.org/10.1021/acsomega.1c00527
*ACS Omega* 2021, 6, 7922−7930

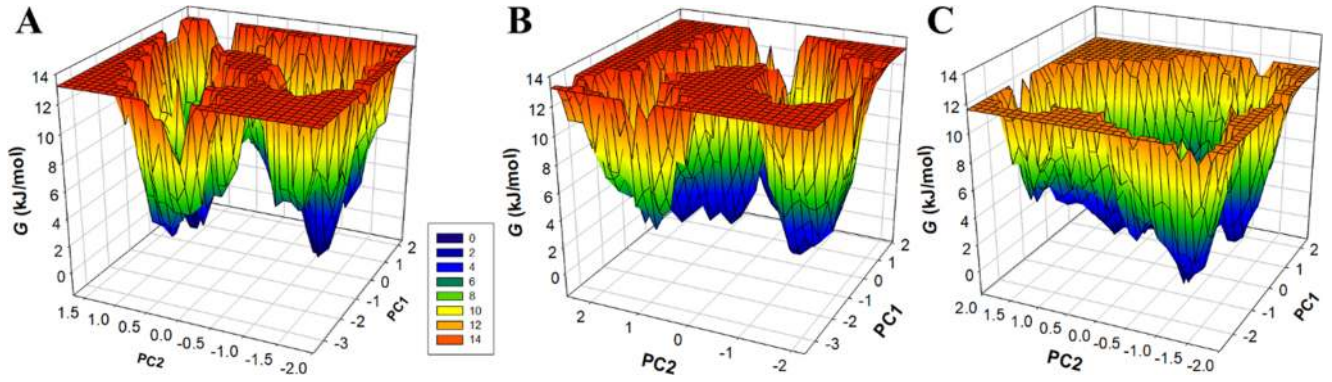


**Figure 7.** The Gibbs energy landscapes were obtained during 100 ns MD simulation for (a) free ferritin, (b) ferritin−quercetin complex, and (c) ferritin−naringenin complex.

explained the stable binding of quercetin and naringenin with ferritin without inducing any significant conformational changes throughout the trajectory. We proposed that the studied natural compounds quercetin and naringenin can further be explored as potential leads targeting ferritin to develop therapeutics for AD treatment.

## 4. MATERIALS AND METHODS

**4.1. Computational Resources.** To perform computer-assisted molecular docking and simulation studies, several bioinformatics tools such as InstaDock,[52] Discovery Studio Visualizer,[53] and GROMACS suite[54] were utilized on a DELL Tower 7810 workstation. For visualization and analysis purposes, PyMOL,[55] Visual Molecular Dynamics,[56] SwissPDB Viewer,[57] and QtGrace[58] were utilized. Several web-based tools and resources such as the RCSB Protein Data Bank (PDB),[59] ZINC database,[60] SwissADME,[61] and PRODRG[62] were utilized in data retrieval, evaluation, and analysis. The three-dimensional structural coordinates of human ferritin with resolution of 1.52 Å were downloaded from the PDB with the identifier 3AJO.[49] The structure was refined further using Swiss PDB-Viewer[57] and M.G.L. AutoDock tools.[63] Three-dimensional structures of quercetin and naringenin were downloaded from the PubChem database.[64]

**4.2. Molecular Docking.** Three-dimensional coordinates of the human ferritin structure were downloaded from the PDB (PDB ID: 3AJO, resolution: 1.52 Å). All heteroatoms including water molecules were deleted from the parent structure and refined further using the Swiss-PDB Viewer and the M.G.L. AutoDock tools. The energy minimization was carried out in vacuo with the GROMOS 43B1 force field in the Swiss-PDB Viewer prior to the docking study. The energy was found to be −9415.97 and −12,417.81 kJ/mol before and after energy minimization, respectively. InstaDock was used for docking where the search space was blind for quercetin and naringenin with a grid size of 50, 50, and 60 Å, centralized at 39.11, −9.80, and 29.02 for $x$, $y$, and $z$ coordinates, respectively. InstaDock uses QuickVina-W, a modified and faster version of AutoDock Vina. The structural coordinates of quercetin and naringenin were downloaded from the PubChem database with compound CID 5280343 and 932, respectively. The docking result was screened for higher binding affinity. All docked conformations of docked quercetin and naringenin were then split through the "splitter" module in InstaDock and further analyzed using PyMOL and Discovery Studio Visualizer for their detailed interaction with ferritin. Here, we have carefully chosen the docked poses of quercetin and naringenin, which critically interact with essential residues of ferritin.

We have also calculated the inhibition constant (p$Ki$), which is a negative decimal logarithm of the inhibition constant that comes from the $\Delta G$ parameter of the docking result. The p$Ki$ value of both compounds was calculated using the following formulae:

$$\Delta G = RT(\mathrm{Ln}Ki_{\mathrm{pred}}) \quad (1)$$

$$Ki_{\mathrm{pred}} = e^{(\Delta G/RT)} \quad (2)$$

$$\mathrm{p}K_i = -\log(Ki_{\mathrm{pred}}) \quad (3)$$

where $\Delta G$ is the binding affinity (kcal/mol); $R$ is the gas constant, 1.98 cal*(mol*K)$^{-1}$; $T$ is the room temperature, 298.15 K; and pred indicates predicted.

Ligand efficiency (LE) is one of the useful parameters used in lead selection by comparing the values of average binding energy per atom.[65] Here, we calculated the LE of quercetin and naringenin utilizing the following formula:

$$\mathrm{LE} = -\Delta G/N$$

where LE is the ligand efficiency (kcal mol$^{-1}$ non-H atom$^{-1}$), $\Delta G$ is the binding affinity (kcal/mol), and $N$ is the number of nonhydrogen atoms in the ligand molecule.

**4.3. MD Simulations.** MD simulations were carried out on the apo ferritin and ferritin−ligand complexes (ferritin−quercetin and ferritin−naringenin) using the GROMOS 54A7 force field implemented in GROMACS-2020. The quercetin and naringenin parameters were generated utilizing the PRODRG server. Each protein−ligand complex was centralized in a virtual cubic box with a 10 Å distance to the edges and solvated in the TIP3P model. An appropriate number of counterions ($Na^+$ and $Cl^-$) were added for neutralization. The resulting systems were energy-minimized by the steepest descent approach for 5000 steps to avoid any steric clashes in the systems. The NVT ensemble and NPT ensemble equilibration was performed for 200 ps at a temperature of 300 K and pressure of 1 bar for each system. The integration steps were set at 2 fs, where snapshots were recorded at every 10 ps for 100 ns of simulation. This simulation was performed on a DELL Tower 7810 machine enabled by Ubuntu 2020. The resulting MD trajectories were utilized through the inbuilt tools of GROMACS for analysis purposes. The visualization and graph plotting were done using


https://dx.doi.org/10.1021/acsomega.1c00527
ACS Omega 2021, 6, 7922−7930

VMD (Visual Molecular Dynamics) and QtGrace tools. PCA and FEL analyses were performed using the *gmx covar* and *gmx-sham* utilities of GROMACS.

**4.4. Principal Component Analysis.** Proteins regulate their functions via entering in different conformations. The overall conformational change is governed by the collective movements of the atoms in a protein. To explore the conformational changes in ferritin, ferritin−quercetin, and ferritin−naringenin docked complex, PCA was carried out utilizing the essential dynamics (ED) approach. To examine the collective motion of ferritin and its docked complexes with quercetin and naringenin occupied in the conformational subspace during the simulation, this approach employs the calculation of the covariance matrix by the projection of the first two principal components (PCs), PC1 and PC2, using the following formula:[66]

$$C_{ij} = <(x_i - <x_i>)(x_j - <x_j>)>$$

where $x_i/x_j$ is the coordinate of the $i^{th}/j^{th}$ atom of the protein and <−> is the ensemble average.

The FELs are explored to understand the folding/unfolding behavior of a protein by examining structural conformations near the native state.[67] We utilized a conformational sampling approach to get FELs to attain apo ferritin, ferritin−quercetin, and ferritin−naringenin docked complex to examine their folding stability and native states. The FELs were generated using conformational sampling through the following calculation:

$$\Delta G(X) = -K_B T \ln P(X)$$

where $K_B$ represents the Boltzmann constant, $T$ represents temperature, and $P(X)$ represents the probability distribution of the system along with the PCs.

## AUTHOR INFORMATION


### Corresponding Author

**Anas Shamsi** − *Centre for Interdisciplinary Research in Basic Sciences, Jamia Millia Islamia, New Delhi 110025, India; Centre of Medical and Bio-Allied Health Sciences Research, Ajman University, Ajman, UAE;* orcid.org/0000-0001-7055-7056; Phone: +91-8266852171; Email: mshamsi1@jmi.ac.in

### Authors

**Moyad Shahwan** − *Centre of Medical and Bio-Allied Health Sciences Research and College of Pharmacy & Health Sciences, Ajman University, Ajman, UAE*

**Mohd Shahnawaz Khan** − *Protein Research Chair, Department of Biochemistry, College of Sciences, King Saud University, Riyadh 11451, Saudi Arabia;* orcid.org/0000-0002-4599-5924

**Fohad Mabood Husain** − *Department of Food Science and Nutrition, Faculty of Food and Agricultural Sciences, King Saud University, Riyadh 11451, Saudi Arabia*

**Fahad A. Alhumaydhi** − *Department of Medical Laboratories, College of Applied Medical Sciences, Qassim University, Buraydah 52571, Saudi Arabia;* orcid.org/0000-0002-0151-8309

**Abdullah S. M. Aljohani** − *Department of Veterinary Medicine, College of Agriculture and Veterinary medicine, Qassim University, Buraydah 52571, Saudi Arabia*

**Md. Tabish Rehman** − *Department of Pharmacognosy, College of Pharmacy, King Saud University, Riyadh 11451, Saudi Arabia*

**Md. Imtaiyaz Hassan** − *Centre for Interdisciplinary Research in Basic Sciences, Jamia Millia Islamia, New Delhi 110025, India;* orcid.org/0000-0002-3663-4940

**Asimul Islam** − *Centre for Interdisciplinary Research in Basic Sciences, Jamia Millia Islamia, New Delhi 110025, India;* orcid.org/0000-0001-9060-7970

Complete contact information is available at: https://pubs.acs.org/10.1021/acsomega.1c00527


### Author Contributions

Conceptualization was done by A.S. and M.S. Methodology was done by A.S., M.S.K., F.M.H., and F.A.A. The software part was done by A.S. and M.T.R. Validation was done by A.S., A.I., and M.I.H. The formal analysis was done by A.S., A.I., and M.I.H. Investigation was done by A.S. and M.S. The resource part was done by A.I. and M.I.H. Data curation was done by A.S., M.S., and M.S.K. Writing of original draft preparation was done by A.S. and M.S. Writing review and editing were done by A.I. and M.I.H. The visualization part was done by A.S.

### Notes

The authors declare no competing financial interest.

## ACKNOWLEDGMENTS

M.S.K., F.M.H., and M.T.R. acknowledge the generous support from the Deanship of Scientific Research at King Saud University, Riyadh, Kingdom of Saudi Arabia (Grant RGP-215).

## REFERENCES


(1) Muhoberac, B. B.; Vidal, R. Abnormal iron homeostasis and neurodegeneration. *Front. Aging Neurosci.* **2013**, *5*, 32.

(2) Wolozin, B.; Golts, N. Book review: iron and Parkinson's disease. *Neuroscientist* **2002**, *8*, 22−32.

(3) Theillet, F.-X.; Binolfi, A.; Bekei, B.; Martorana, A.; Rose, H. M.; Stuiver, M.; Verzini, S.; Lorenz, D.; Van Rossum, M.; Goldfarb, D. Structural disorder of monomeric α-synuclein persists in mammalian cells. *Nature* **2016**, *530*, 45−50.

(4) Liu, J.-L.; Fan, Y.-G.; Yang, Z.-S.; Wang, Z.-Y.; Guo, C. Iron and Alzheimer's disease: from pathogenesis to therapeutic implications. *Front. Aging Neurosci.* **2018**, *12*, 632.

(5) Hands, S.; Sajjad, M. U.; Newton, M. J.; Wyttenbach, A. In vitro and in vivo aggregation of a fragment of huntingtin protein directly causes free radical production. *J. Biol. Chem.* **2011**, *286*, 44512−44520.

(6) Rouault, T. A. Iron metabolism in the CNS: implications for neurodegenerative diseases. *Nat. Rev. Neurosci.* **2013**, *14*, 551−564.

(7) Meyer, E.; Kurian, M. A.; Hayflick, S. J. Neurodegeneration with brain iron accumulation: genetic diversity and pathophysiological mechanisms. *Annu. Rev. Genomics Hum. Genet.* **2015**, *16*, 257−279.

(8) Oshiro, S.; Morioka, M. S.; Kikuchi, M. Dysregulation of iron metabolism in Alzheimer's disease, Parkinson's disease, and amyotrophic lateral sclerosis. *Adv. Pharmacol. Sci.* **2011**, *2011*, 1.

(9) Crichton, R. R.; Declercq, J.-P. X-ray structures of ferritins and related proteins. *Biochim. Biophys. Acta, Gen. Subj.* **2010**, *1800*, 706−718.

(10) Harrison, P. M.; Arosio, P. The ferritins: molecular properties, iron storage function and cellular regulation. *Biochim. Biophys. Acta, Bioenerg.* **1996**, *1275*, 161−203.

(11) Chasteen, N. Ferritin. Uptake, storage, and release of iron. *Met. Ions Biol. Syst.* **1998**, *35*, 479−514.

(12) Cheng, X.-S.; Zhao, K.-P.; Jiang, X.; Du, L.-L.; Li, X.-H.; Ma, Z.-W.; Yao, J.; Luo, Y.; Duan, D.-X.; Wang, J.-Z. Nmnat2 attenuates Tau

phosphorylation through activation of PP2A. *J. Alzheimer's Dis.* **2013**, *36*, 185−195.
(13) Kumar, A.; Nisha, C. M.; Silakari, C.; Sharma, I.; Anusha, K.; Gupta, N.; Nair, P.; Tripathi, T.; Kumar, A. Current and novel therapeutic molecules and targets in Alzheimer's disease. *J. Formosan Med. Assoc.* **2016**, *115*, 3−10.
(14) Ikonomovic, M.; Klunk, W.; Abrahamson, E.; Wuu, J.; Mathis, C.; Scheff, S.; Mufson, E.; DeKosky, S. Precuneus amyloid burden is associated with reduced cholinergic activity in Alzheimer disease. *Neurology* **2011**, *77*, 39−47.
(15) Tripathi, T.; Khan, H. Direct Interaction between the $\beta$-Amyloid Core and Tau Facilitates Cross-Seeding: A Novel Target for Therapeutic Intervention. *Biochemistry* **2020**, *59*, 341−342.
(16) Cunningham, C.; Wilcockson, D. C.; Campion, S.; Lunnon, K.; Perry, V. H. Central and systemic endotoxin challenges exacerbate the local inflammatory response and increase neuronal death during chronic neurodegeneration. *J. Neurosci.* **2005**, *25*, 9275−9284.
(17) Martins, C.; Galetti, P. M. Chromosomal localization of 5S rDNA genes in Leporinus fish (Anostomidae, Characiformes). *Chromosome Res.* **1999**, *7*, 363−367.
(18) Nunomura, A.; Perry, G.; Aliev, G.; Hirai, K.; Takeda, A.; Balraj, E. K.; Jones, P. K.; Ghanbari, H.; Wataya, T.; Shimohama, S. Oxidative damage is the earliest event in Alzheimer disease. *J. Neuropathol. Exp. Neurol.* **2001**, *60*, 759−767.
(19) Wang, P.; Wang, Z.-Y. Metal ions influx is a double edged sword for the pathogenesis of Alzheimer's disease. *Ageing Res. Rev.* **2017**, *35*, 265−290.
(20) Lovell, M.; Robertson, J.; Teesdale, W.; Campbell, J.; Markesbery, W. Copper, iron and zinc in Alzheimer's disease senile plaques. *J. Neurol. Sci.* **1998**, *158*, 47−52.
(21) Ashraf, M. G.; Greig, N. H.; Khan, T. A.; Hassan, I.; Tabrez, S.; Shakil, S.; Sheikh, I. A.; Zaidi, S. K.; Akram, M.; Jabir, N. R. Protein misfolding and aggregation in Alzheimer's disease and type 2 diabetes mellitus. *CNS Neurol. Disord.: Drug Targets* **2014**, *13*, 1280−1293.
(22) Myhre, O.; Utkilen, H.; Duale, N.; Brunborg, G.; Hofer, T. Metal dyshomeostasis and inflammation in Alzheimer's and Parkinson's diseases: possible impact of environmental exposures. *Oxid. Med. Cell. Longevity* **2013**, *2013*, 1.
(23) Wright, R. O.; Baccarelli, A. Metals and neurotoxicology. *J. Nutr.* **2007**, *137*, 2809−2813.
(24) Goozee, K.; Chatterjee, P.; James, I.; Shen, K.; Sohrabi, H. R.; Asih, P. R.; Dave, P.; Manyan, C.; Taddei, K.; Ayton, S. J. Elevated plasma ferritin in elderly individuals with high neocortical amyloid-$\beta$ load. *Mol. Psychiatry* **2018**, *23*, 1807−1812.
(25) Meadowcroft, M. D.; Connor, J. R.; Smith, M. B.; Yang, Q. X. MRI and histological analysis of beta-amyloid plaques in both human Alzheimer's disease and APP/PS1 transgenic mice. *J. Magn. Reson. Imaging* **2009**, *29*, 997−1007.
(26) Smith, M. A.; Harris, P. L. R.; Sayre, L. M.; Perry, G. Iron accumulation in Alzheimer disease is a source of redox-generated free radicals. *Proc. Natl. Acad. Sci.* **1997**, *94*, 9866−9868.
(27) Spencer, J. P. E. Flavonoids: modulators of brain function? *Br. J. Nutr.* **2008**, *99*, ES60−ES77.
(28) Vafeiadou, K.; Vauzour, D.; Spencer, J. Neuroinflammation and its modulation by flavonoids. *Endocrine, Metabolic & Immune Disorders-Drug Targets (Formerly Current Drug Targets-Immune, Endocrine & Metabolic Disorders)* **2007**, *7*, 211−224.
(29) Vauzour, D.; Vafeiadou, K.; Rodriguez-Mateos, A.; Rendeiro, C.; Spencer, J. P. The neuroprotective potential of flavonoids: a multiplicity of effects. *Genes Nutr.* **2008**, *3*, 115−126.
(30) Abd El Mohsen, M. M.; Kuhnle, G.; Rechner, A. R.; Schroeter, H.; Rose, S.; Jenner, P.; Rice-Evans, C. A. Uptake and metabolism of epicatechin and its access to the brain after oral ingestion. *Free Radical Biol. Med.* **2002**, *33*, 1693−1702.
(31) Benavente-García, O.; Castillo, J.; Marin, F. R.; Ortuño, A.; Del Río, J. A. Uses and properties of citrus flavonoids. *J. Agric. Food Chem.* **1997**, *45*, 4505−4515.
(32) Middleton, E., Jr. The impact of plant flavonoids on mammalian biology: implications for immunity, inflammation and cancer. *The flavonoids: advances in research since 1993*; Routledge 1986, 337 −370.
(33) Montanari, A.; Chen, J.; Widmer, W. Citrus flavonoids: a review of past biological activity against disease. *Flavonoids in the living system* **1998**, 103−116.
(34) Ortuno, A.; Garcia-Puig, D.; Fuster, M. D.; Perez, M. L.; Sabater, F.; Porras, I.; Garcia-Lidon, A.; Del Rio, J. A. Flavanone and nootkatone levels in different varieties of grapefruit and pummelo. *J. Agric. Food Chem.* **1995**, *43*, 1−5.
(35) Vafeiadou, K.; Vauzour, D.; Lee, H. Y.; Rodriguez-Mateos, A.; Williams, R. J.; Spencer, J. P. E. The citrus flavanone naringenin inhibits inflammatory signalling in glial cells and protects against neuroinflammatory injury. *Arch. Biochem. Biophys.* **2009**, *484*, 100−109.
(36) Heo, H. J.; Kim, D.-O.; Shin, S. C.; Kim, M. J.; Kim, B. G.; Shin, D.-H. Effect of antioxidant flavanone, naringenin, from Citrus junos on neuroprotection. *J. Agric. Food Chem.* **2004**, *52*, 1520−1525.
(37) Bragg, P. D.; Rainnie, D. J. The effect of silver ions on the respiratory chain of Escherichia coli. *Can. J. Microbiol.* **1974**, *20*, 883−889.
(38) Zbarsky, V.; Datla, K. P.; Parkar, S.; Rai, D. K.; Aruoma, O. I.; Dexter, D. T. Neuroprotective properties of the natural phenolic antioxidants curcumin and naringenin but not quercetin and fisetin in a 6-OHDA model of Parkinson's disease. *Free Radical Res.* **2005**, *39*, 1119−1125.
(39) Mani, S.; Sekar, S.; Barathidasan, R.; Manivasagam, T.; Thenmozhi, A. J.; Sevanan, M.; Chidambaram, S. B.; Essa, M. M.; Guillemin, G. J.; Sakharkar, M. K. Naringenin decreases $\alpha$-synuclein expression and neuroinflammation in MPTP-induced Parkinson's disease model in mice. *Neurotoxic. Res.* **2018**, *33*, 656−670.
(40) Rogerio, A. P.; Kanashiro, A.; Fontanari, C.; Da Silva, E. V. G.; Lucisano-Valim, Y. M.; Soares, E. G.; Faccioli, L. H. Anti-inflammatory activity of quercetin and isoquercitrin in experimental murine allergic asthma. *Inflammation Res.* **2007**, *56*, 402−408.
(41) Lamson, D. W.; Brignall, M. S. Antioxidants and cancer, part 3: quercetin. *Altern. Med. Rev.* **2000**, *5*, 196−208.
(42) Youdim, K. A.; Qaiser, M. Z.; Begley, D. J.; Rice-Evans, C. A.; Abbott, N. J. Flavonoid permeability across an in situ model of the blood−brain barrier. *Free Radical Biol. Med.* **2004**, *36*, 592−604.
(43) Heo, H. J.; Lee, C. Y. Protective effects of quercetin and vitamin C against oxidative stress-induced neurodegeneration. *J. Agric. Food Chem.* **2004**, *52*, 7514−7517.
(44) Uddin, M.; Kabir, M.; Rahman, M.; Behl, T.; Jeandet, P.; Ashraf, G. M.; Najda, A.; Bin-Jumah, M. N.; El-Seedi, H. R.; Abdel-Daim, M. M. Revisiting the amyloid cascade hypothesis: From anti-A$\beta$ therapeutics to auspicious new ways for Alzheimer's disease. *Int. J. Mol. Sci.* **2020**, *21*, 5858.
(45) Mahesh, T.; Menon, V. P. Quercetin allievates oxidative stress in streptozotocin-induced diabetic rats. *Phytother. Res.* **2004**, *18*, 123−127.
(46) Fiorani, M.; de Sanctis, R.; Menghinello, P.; Cucchiarini, L.; Cellini, B.; Dachá, M. Quercetin prevents glutathione depletion induced by dehydroascorbic acid in rabbit red blood cells. *Free Radic Res.* **2001**, *34*, 639−648.
(47) Pu, F.; Mishima, K.; Irie, K.; Motohashi, K.; Tanaka, Y.; Orito, K.; Egawa, T.; Kitamura, Y.; Egashira, N.; Iwasaki, K.; Fujiwara, M. Neuroprotective effects of quercetin and rutin on spatial memory impairment in an 8-arm radial maze task and neuronal death induced by repeated cerebral ischemia in rats. *J. Pharmacol. Sci.* **2007**, 329.
(48) Subramanian, V.; Evans, D. G. A molecular dynamics and computational study of ligand docking and electron transfer in ferritins. *The Journal of Physical Chemistry B* **2012**, *116*, 9287−9302.
(49) Masuda, T.; Goto, F.; Yoshihara, T.; Mikami, B. The universal mechanism for iron translocation to the ferroxidase site in ferritin, which is mediated by the well conserved transit site. *Biochem. Biophys. Res. Commun.* **2010**, *400*, 94−99.
(50) Ito, A.; Mukaiyama, A.; Itoh, Y.; Nagase, H.; Thøgersen, I. B.; Enghild, J. J.; Sasaguri, Y.; Mori, Y. Degradation of interleukin 1$\beta$ by matrix metalloproteinases. *J. Biol. Chem.* **1996**, *271*, 14657−14660.


https://dx.doi.org/10.1021/acsomega.1c00527
*ACS Omega* 2021, 6, 7922−7930

(51) Hubbard, R. E.; Kamran Haider, M., Hydrogen Bonds in Proteins: Role and Strength; In *eLS*; John Wiley & Sons, Ltd: 2001.
(52) Mohammad, T.; Mathur, Y.; Hassan, M. I. InstaDock: A single-click graphical user interface for molecular docking-based virtual high-throughput screening. *Briefings Bioinf.* **2020**, bbaa279.
(53) Biovia, D. S. *Discovery studio modeling environment*. San Diego: Dassault Systèmes 2015.
(54) Abraham, M. J.; Murtola, T.; Schulz, R.; Páll, S.; Smith, J. C.; Hess, B.; Lindahl, E. GROMACS: High performance molecular simulations through multi-level parallelism from laptops to supercomputers. *SoftwareX* **2015**, *1-2*, 19−25.
(55) DeLano, W. L. Pymol: An open-source molecular graphics tool. *CCP4 Newsletter on protein crystallography;* Citeseer 2002, *40* (1), 82−92.
(56) Humphrey, W.; Dalke, A.; Schulten, K. VMD: visual molecular dynamics. *J. Mol. Graphics* **1996**, *14*, 33−38.
(57) Guex, N.; Peitsch, M. C. SWISS-MODEL and the Swiss-Pdb Viewer: an environment for comparative protein modeling. *Electrophoresis* **1997**, *18*, 2714−2723.
(58) Turner, P., Grace-5.1. 22/qtGrace v 0.2. 4. 2018.
(59) Berman, H. M.; Bourne, P. E.; Westbrook, J.; Zardecki, C., The protein data bank. In *Protein Structure*; CRC Press: 2003; pp. 394−410.
(60) Sterling, T.; Irwin, J. J. ZINC 15−ligand discovery for everyone. *J. Chem. Inf. Model.* **2015**, *55*, 2324−2337.
(61) Daina, A.; Michielin, O.; Zoete, V. SwissADME: a free web tool to evaluate pharmacokinetics, drug-likeness and medicinal chemistry friendliness of small molecules. *Sci. Rep.* **2017**, *7*, 42717.
(62) Van Aalten, D. M. F.; Bywater, R.; Findlay, J. B. C.; Hendlich, M.; Hooft, R. W. W.; Vriend, G. PRODRG, a program for generating molecular topologies and unique molecular descriptors from coordinates of small molecules. *J. Comput.-Aided Mol. Des.* **1996**, *10*, 255−262.
(63) Forli, S.; Huey, R.; Pique, M. E.; Sanner, M. F.; Goodsell, D. S.; Olson, A. J. Computational protein−ligand docking and virtual drug screening with the AutoDock suite. *Nat. Protoc.* **2016**, *11*, 905−919.
(64) Kim, S.; Thiessen, P. A.; Bolton, E. E.; Chen, J.; Fu, G.; Gindulyte, A.; Han, L.; He, J.; He, S.; Shoemaker, B. A.; Wang, J.; Yu, B.; Zhang, J.; Bryant, S. H. PubChem substance and compound databases. *Nucleic Acids Res.* **2016**, *44*, D1202−D1213.
(65) Hopkins, A. L.; Groom, C. R.; Alex, A. Ligand efficiency: a useful metric for lead selection. *Drug Discovery Today* **2004**, *9*, 430.
(66) Altis, A.; Otten, M.; Nguyen, P. H.; Hegger, R.; Stock, G. Construction of the free energy landscape of biomolecules via dihedral angle principal component analysis. *J. Chem. Phys.* **2008**, *128*, No. 06B620.
(67) Papaleo, E.; Mereghetti, P.; Fantucci, P.; Grandori, R.; De Gioia, L. Free-energy landscape, principal component analysis, and structural clustering to identify representative conformations from molecular dynamics simulations: the myoglobin case. *J. Mol. Graphics Modell.* **2009**, *27*, 889−899.


https://dx.doi.org/10.1021/acsomega.1c00527
*ACS Omega* 2021, 6, 7922−7930